Electronic Supplementary Information

An efficient mixed-valence copper pyrazolate catalyst for the conversion of carbon dioxide and epoxides into cyclic carbonates

Jian-Ge Wang,‡[a] Yang Liu,‡[b] Chun-Mei Liu,[a] Jing-Huo Chen[*a] and Guang Yang[*a]

[a]Green Catalysis Center, and College of Chemistry, Zhengzhou University, Zhengzhou, Henan, 450001, China.
[b]Henan Technician College of Medicine and Health, Kaifeng, Henan, 475000, China.

‡These authors contributed equally.

*Corresponding author.
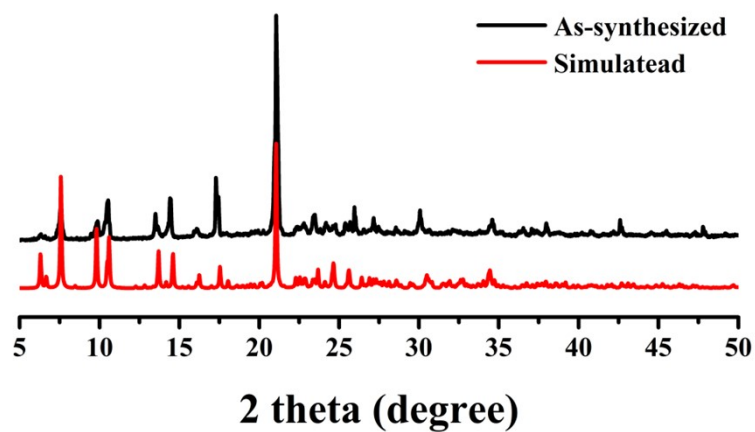E-mail address: jhchen@zzu.edu.cn; yang@zzu.edu.cn

Figure S1. The P-XRD patterns of **1** obtained from the as-synthesized sample (black line) and the simulation based on the crystal data (red line).
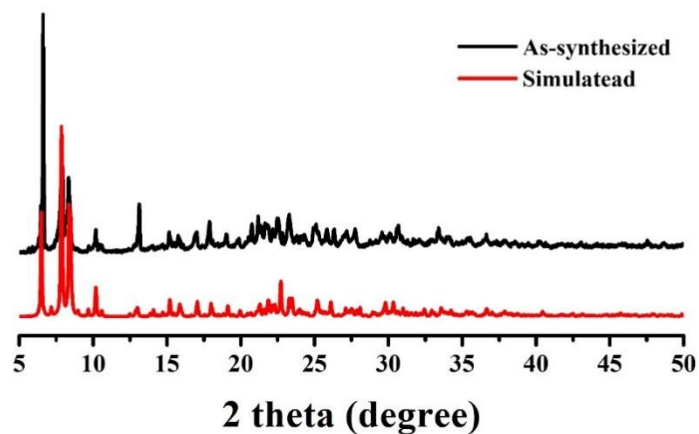

Figure S2. The P-XRD patterns of **2** obtained from the as-synthesized sample (black line) and the simulation based on the crystal data (red line).
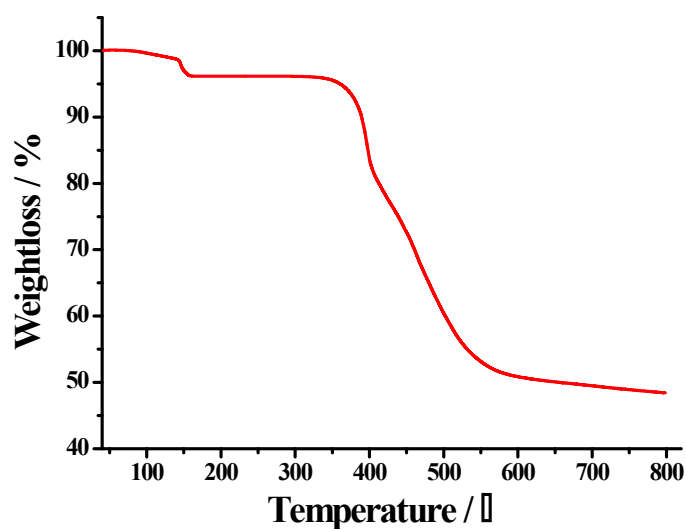

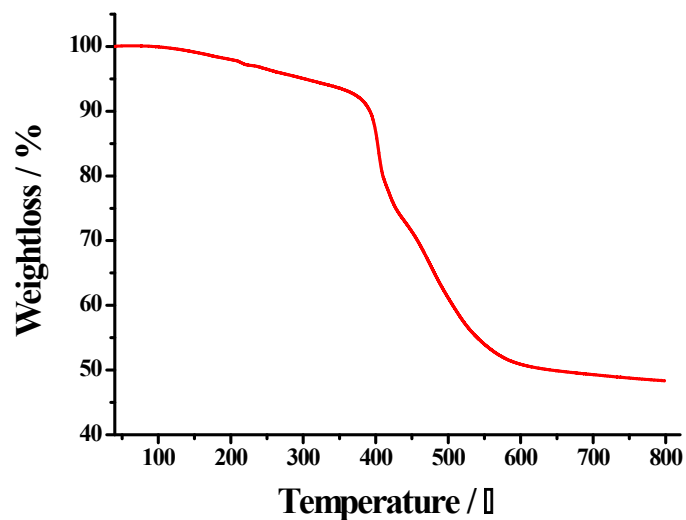**Figure S3.** Thermogravimetric curve of **1**.
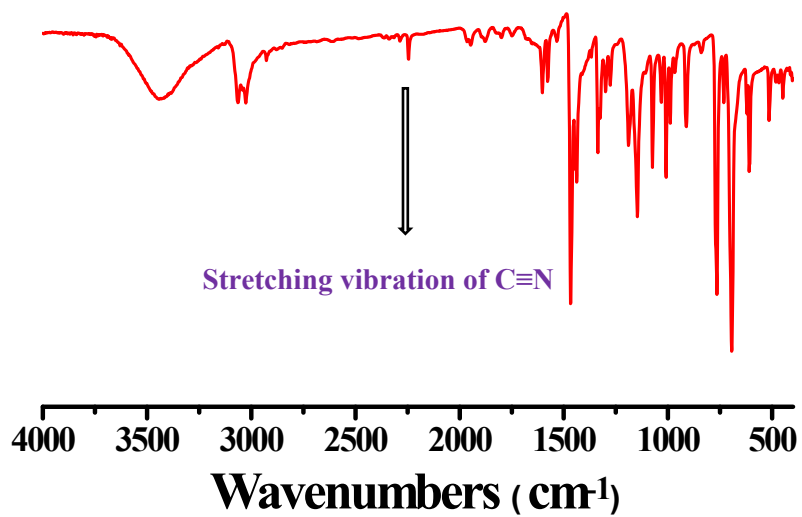
Figure S4. Thermogravimetric curve of **2**.

Stretching vibration of C≡N

Figure S5. IR spectrum of **1** as KBr pellet.
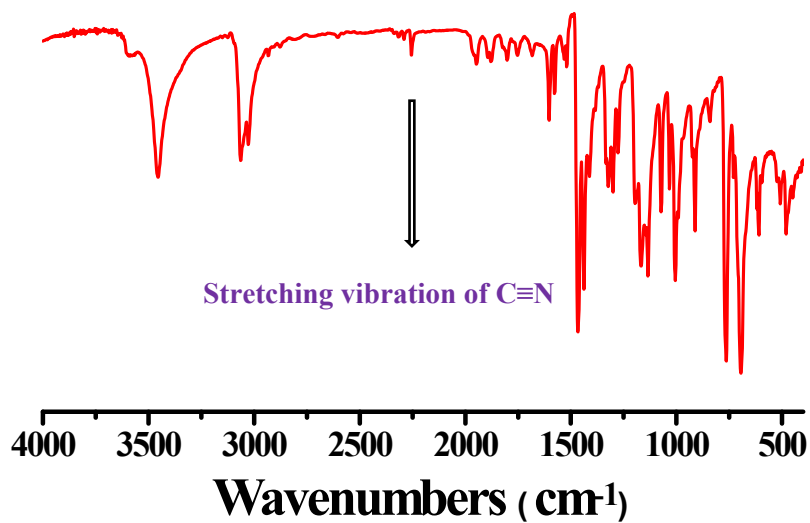

Stretching vibration of C≡N
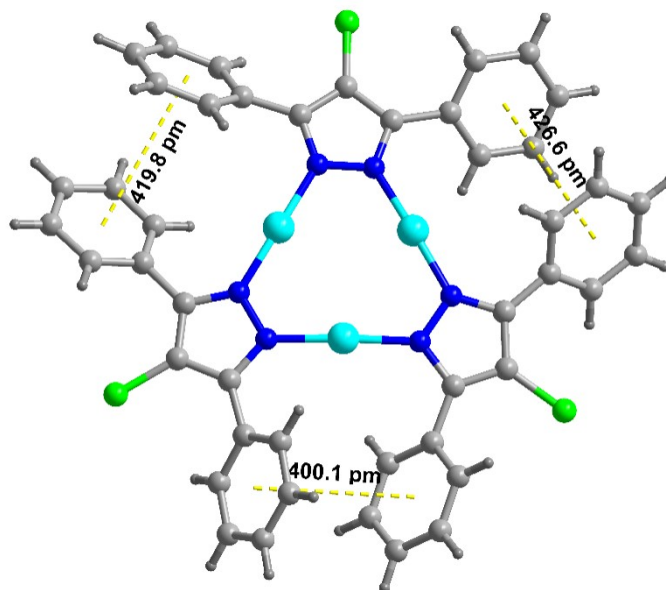
Figure S6. IR spectrum of **2** as KBr pellet.

Figure S7. The intramolecular π(Ph)$\cdots\pi$(Ph) interaction in **1**, CH$_3$CN molecule has been omitted for clarity. Colour code: Cu, turquoise; N, blue; C, light grey; H, dark grey; Cl, bright green.
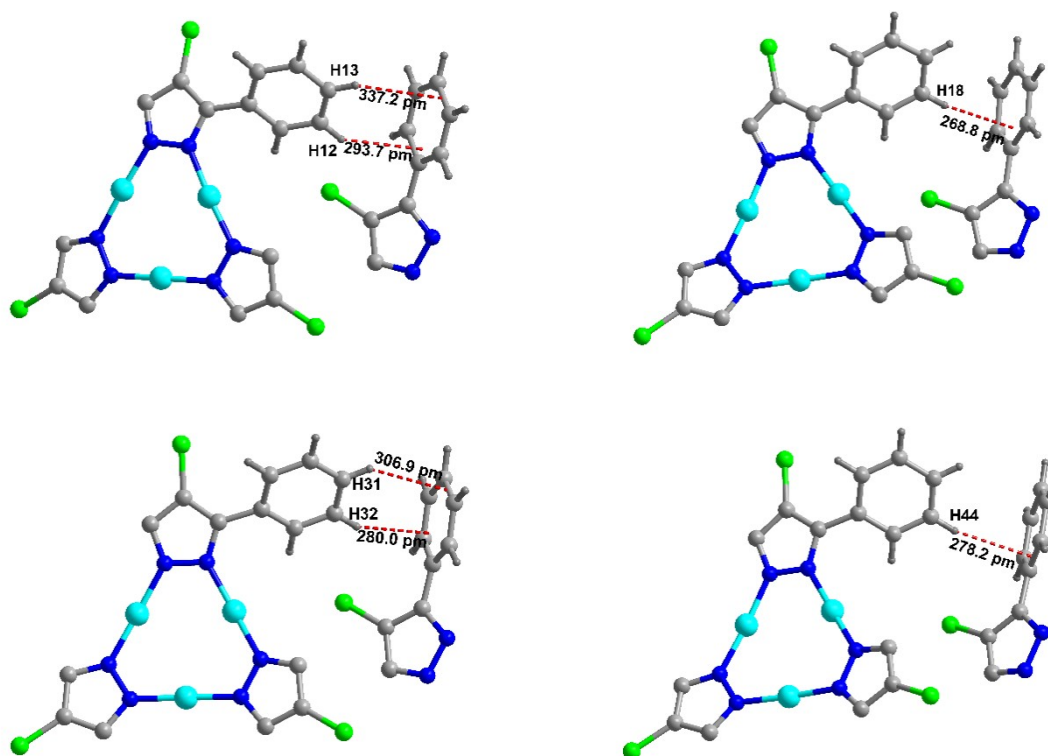

Figure S8. The intermolecular C-H$\cdots\pi$(Ph) interaction in **1**, CH$_3$CN molecule and some phenyl groups have been omitted for clarity. Colour code: Cu, turquoise; O, red; N, blue; C, light grey; H, dark grey; Cl, bright green.

Figure S9. The intermolecular Cl···H(Ph) interactions in **1**, CH$_3$CN molecule and some phenyl groups have been omitted for clarity. Colour code: Cu, turquoise; N, blue; C, light grey; H, dark grey; Cl, bright green.
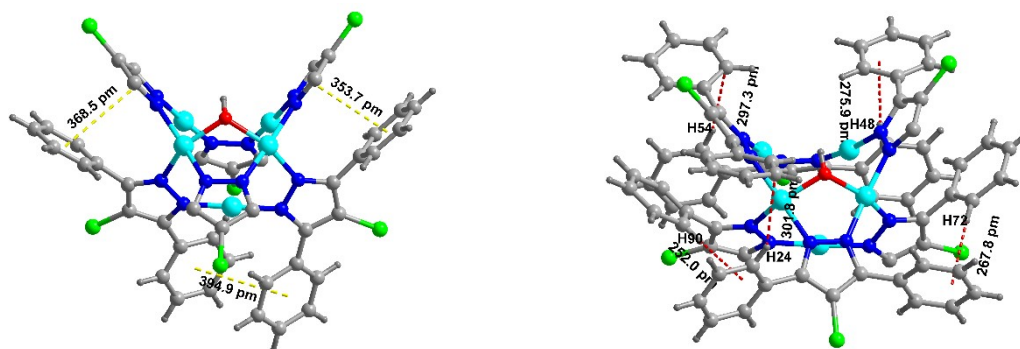
Figure S10. The intramolecular π(Ph)···π(Ph) interaction and C-H···π(Ph) interaction in **2**, CH$_3$CN molecule and some phenyl groups have been omitted for clarity. Colour code: Cu, turquoise; O, red; N, blue; C, light grey; H, dark grey; Cl, bright green.

Figure S11. The intermolecular C-H···π(Ph) interaction in **2**, CH$_3$CN molecule and some phenyl groups have been omitted for clarity. Colour code: Cu, turquoise; O, red; N, blue; C, light grey; H, dark grey; Cl, bright green.
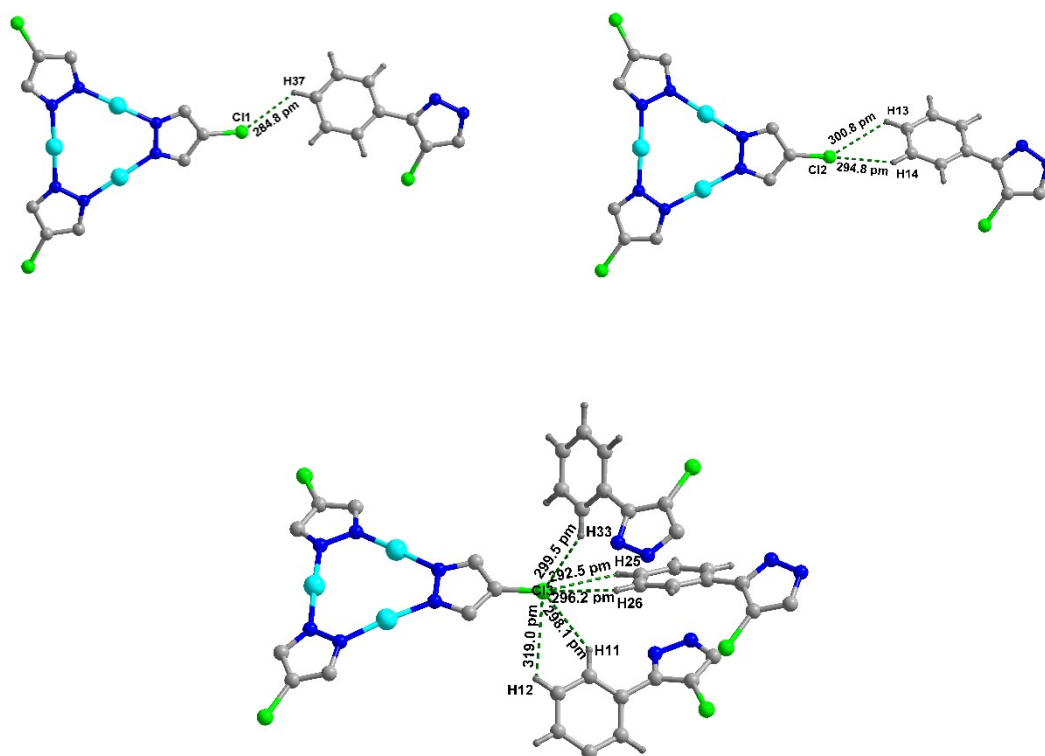
Figure S12. The intermolecular Cl···H(Ph) interactions in **2**, CH₃CN molecule and some phenyl groups have been omitted for clarity. Colour code: Cu, turquoise; O, red; N, blue; C, light grey; H, dark grey; Cl, bright green.
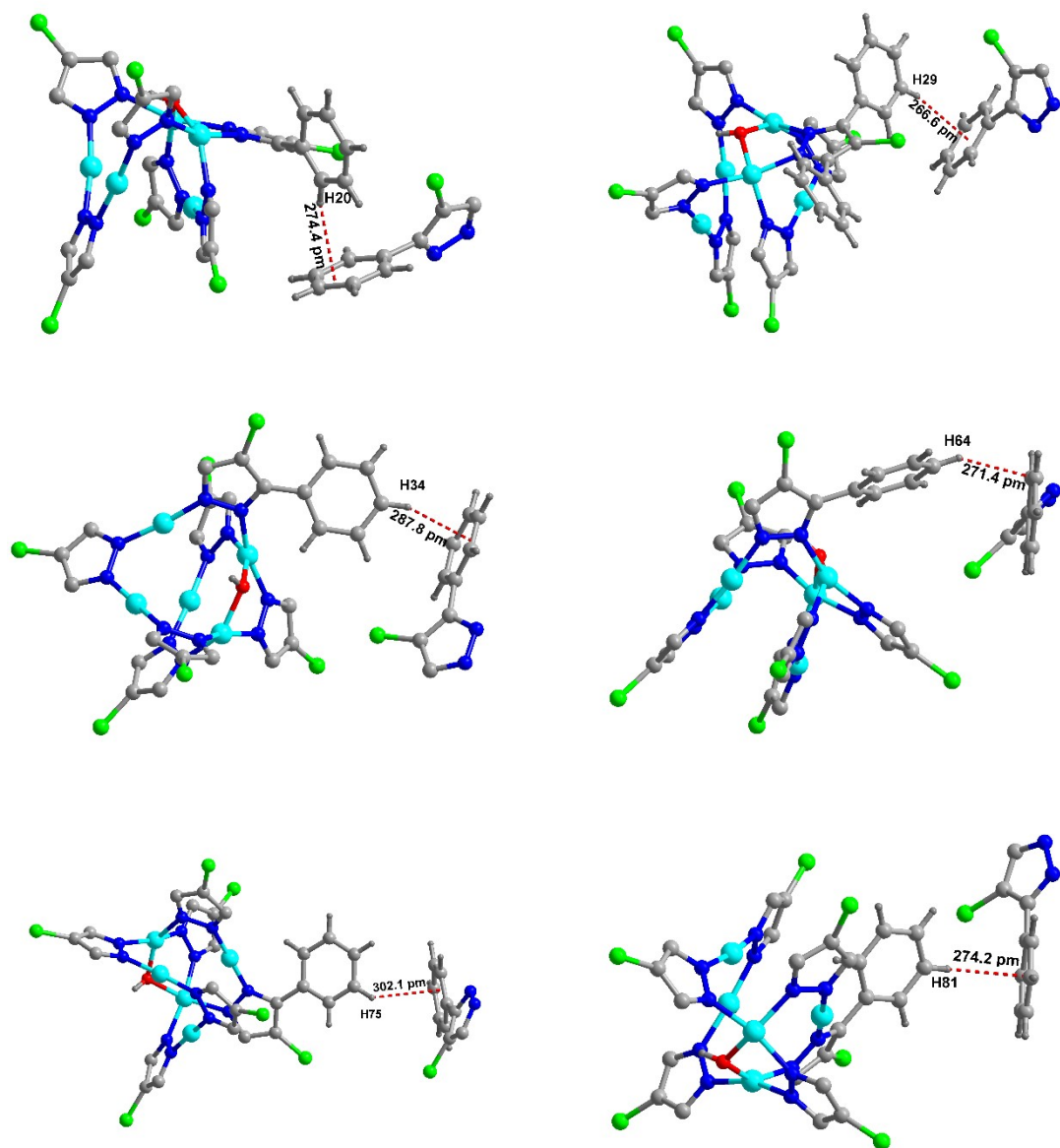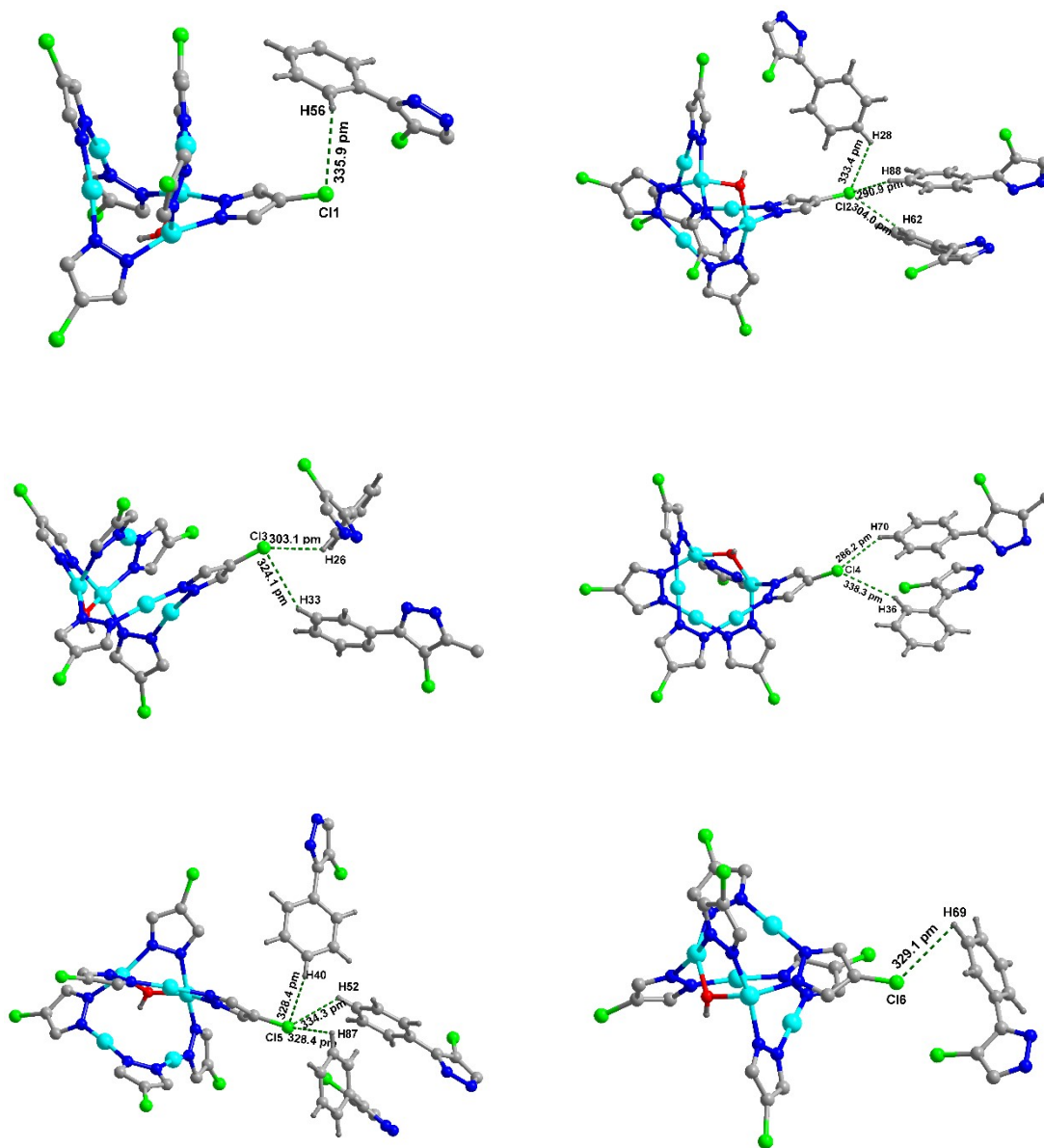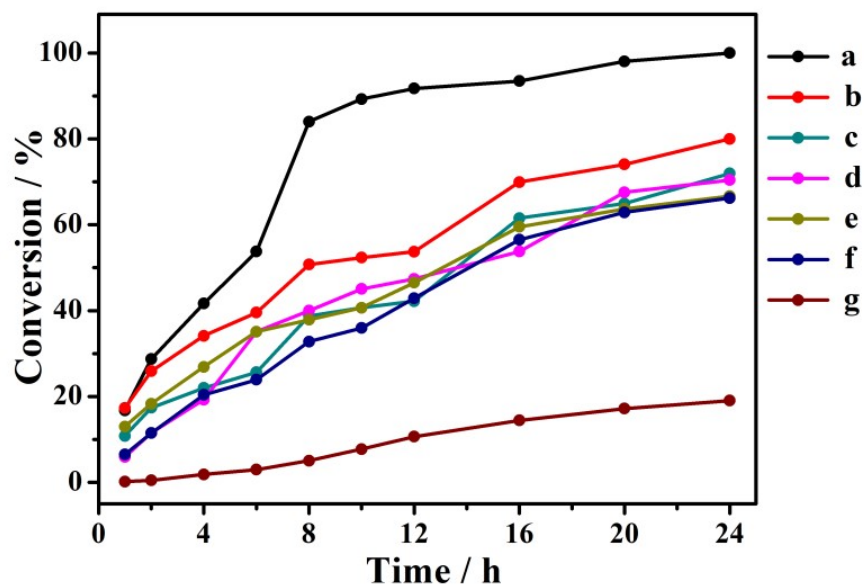
Figure S13. The curves of reaction conversion rate for the formation of propylene carbonate versus time. Reaction conditions: CO_2 (1 atm, using a balloon), propylene oxide (25.0 mmol) with **2** and TBAB (Bu$_4$NBr) as catalysts at 25°C, a: **2** (0.15 mmol), TATB (1.8 mmol); b: **2** (0.1 mmol), TATB (1.8 mmol); c: **2** (0.05 mmol), TATB (1.8 mmol); d: **2** (0.025 mmol), TATB (1.8 mmol); e: **2** (0.15 mmol), TATB (1.2 mmol); f: **2** (0.15 mmol), TATB (0.6 mmol); g: **2** (0 mmol), TATB (1.8 mmol).

Figure S14. Cu 2p XPS spectrum of **1**.

Figure S15. The LUMO and HUMO of **2** obtained by DFT calculation.

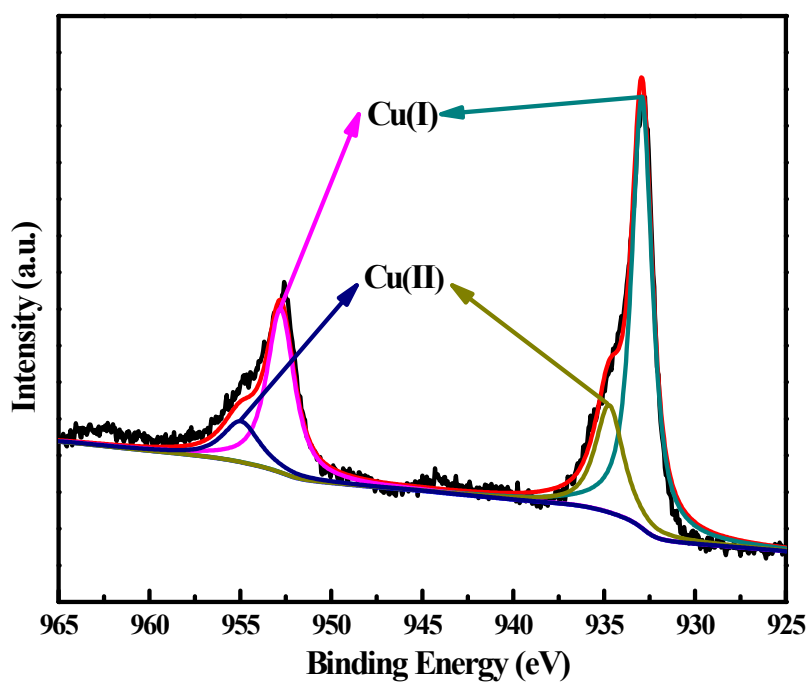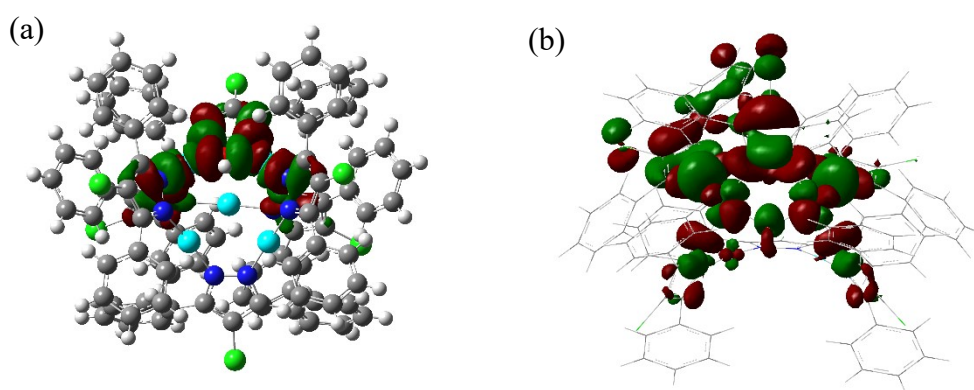**Table S1.** Selected bond distances (Å) and bond angles (º) for **1** and **2**.

1			
Cu(1)-N(2)	1.883(2)	Cu(1)-N(3)	1.883(2)
Cu(2)-N(4)	1.879(2)	Cu(2)-N(6)	1.878(2)
Cu(3)-N(1)	1.868(2)	Cu(3)-N(6)	1.871(2)
N(2)-Cu(1)-N(3)	174.49(10)	N(4)-Cu(1)-N(5)	173.48(10)
N(1)-Cu(1)-N(6)	174.57(10)	Cu(1)···N≡CCH$_3$	2.783(3)
Cu(2)···N≡CCH$_3$	2.853(3)	Cu(3)···N≡CCH$_3$	2.830(3)
2			
Cu(1)-O(1)	1.902(4)	Cu(1)-N(1)	1.978(5)
Cu(1)-N(8)	1.958 (5)	Cu(1)-N(12)	1.985(5)
Cu(2)-O(1)	1.909(4)	Cu(2)-N(2)	1.968(5)
Cu(2)-N(3)	1.954(5)	Cu(2)-N(9)	1.983(5)
Cu(3)-N(4)	1.860(5)	Cu(3)-N(5)	1.867(5)
Cu(4)-N(6)	1.862(5)	Cu(4)-N(7)	1.865(5)
Cu(5)-N(10)	1.874(5)	Cu(5)-N(11)	1.855(5)
O(1)-Cu(1)-N(1)	84.53(19)	O(1)-Cu(1)-N(8)	94.03(19)
O(1)-Cu(1)-N(12)	146.3(2)	N(1)-Cu(1)-N(8)	161.9(2)
N(1)-Cu(1)-N(12)	95.3(2)	N(8)-Cu(1)-N(12)	95.9(2)
O(1)-Cu(2)-N(2)	84.41(19)	O(1)-Cu(2)-N(3)	91.87(19)
O(1)-Cu(2)-N(9)	151.42(19)	N(2)-Cu(2)-N(3)	164.4(2)
N(2)-Cu(2)-N(9)	95.2(2)	N(3)-Cu(2)-N(9)	95.3(2)
N(4)-Cu(3)-N(5)	172.0(2)	N(6)-Cu(4)-N(7)	175.9(2)
N(10)-Cu(5)-N(11)	176.3(2)	Cu(1)-O(1)-Cu(2)	112.7(2)

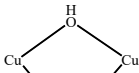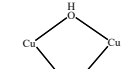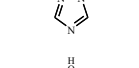**Table S2.** Comparison of structural parameters of Cu^{II}–O–Cu^{II} motifs.
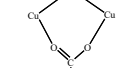
Structural motif	Distance (Å)		Bond angles (°)	CCDC code	Ref.
	$Cu^{II} \cdots Cu^{II}$	Cu^{II}-O	Cu^{II}-O-Cu^{II}		
	3.173	1.902; 1.909	112.7	1975110	This paper
	3.448	1.991; 1.999	119.6	161798	1
	3.257-3.406	1.886-1.945	116.5-125.3	2117298	2
	3.282	1.913; 1.918	118.0	666709	3
	3.417; 3.362	1.936-1.950	119.6; 123.5	1020049	4
	3.357	1.908; 1.913	123.0	2045673	5
	3.227	1.932; 1.939	112.9	1827952	6
	3.199	1.908; 1.910	113.9	1825437	7
	3.213	1.902; 1.920	114.4	1007288	8
	3.331	1.913; 1.880	122.9	2064099	9

Table S3. Comparison of the catalytic activity of **2** with previously reported homogeneous catalysts in the cycloaddition of CO_2 with propylene oxide.

| Entry	Catalyst	Co-catalyst	Pressure	Temp	Time (h)	Yield (%)	Ref.
1	**2**	TBAB	1 atm	R.T.	24	99	This paper
2	$Mo_2(O^tBu)_6$	TBAB	1 atm	R.T.	24	98	10
3	$[Cu_6(\mu_4\text{-}O)_2(SO_4)_4(DMA)_6]$	TBAB	1 atm	R.T.	24	98	11
4	(salen)CoI	2-(Triphenylphosphoranylidene)-acetaldehyde	1 atm	R.T.	24	90	12
5	[urea-Zn]I_2		1.5 MPa	120 °C	3.0	95	13
6	$[AlMe_2\{\kappa_2\text{-mbpzbdeape}\}]I_2$		1 MPa	70 °C	18	78	14
7	$[Fe(BIP^{PrIm})(dhbpy)I]I$	Tetraphenylphosphonium iodide	0.5 MPa	50 °C	20	72	15
8	$[Heemim][ZrCl_5]$		1 MPa	120 °C	3	96	16
9	$[La\{N(SiHMe_2)_2\}_2\{k_3\text{-bpzcp}\}]$	TBAB	1 MPa	70 °C	16	95	17
10	1,8-diazabicyclo[5.4.0]-undec-7-ene	Cellulose	20 atm	120 °C	2	90	18

Abbreviations used:

salen: (1E,1'E)-N,N'-((1R,2R)-cyclohexane-1,2-diyl)bis(1-(3,5-di-*tert*-butyl-2-(l¹-oxidaneyl)phenyl)methanimine

mbpzbdeape: 1,1'-(2,2-bis(4-(diethyl(methyl)-l⁴-azaneyl)phenyl)-2-(l¹-oxidaneyl)ethane-1,1-diyl)bis(3,5-dimethyl-1*H*-pyrazole)

BIP^{PrIm}: (1E,1′E)-1,1′-(4-(benzyloxy)pyridine-2,6-diyl)bis(N-(3-(1*H*-imidazol-1-yl)propyl)methanimine)

dhbpy: [2,2'-bipyridine]-6,6'-diol

Heemim: 1-[2-(2-hydroxyethoxy)ethyl]-3-methylimidazolium

Bpzcp: 2,2-bis(3,5-dimethylpyrazol-1-yl)-1,1-diphe-nylethylcyclopentadienyl
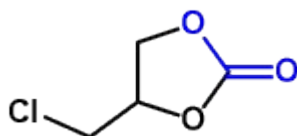
NMR data for products:
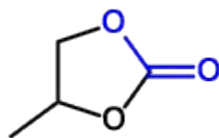
4-methyl-1,3-dioxolan-2-one
^{1}H NMR (400 MHz, CDCl₃): δ 4.86-4.80 (m, 1H), 4.54-4.51 (m, 1H,), 4.01-3.98 (m, 1H), 1.45-1.44 (d, 3H) ppm;
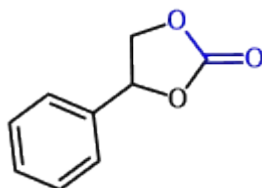**^{13}C NMR (101 MHz, CDCl₃)**: δ 155.11, 73.64, 70.72, 19.40 ppm.

4-(chloromethyl)-1,3-dioxolan-2-one
^{1}H NMR (300 MHz, CDCl₃): δ 4.97 (s, 1H), 4.60-4.56 (t, 1H), 4.41-4.37 (t, 1H), 3.81-3.77 (dd, 1H), 3.73-3.70 (dd, 1H) ppm;
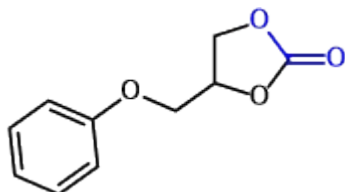**^{13}C NMR (75 MHz, CDCl₃)**: δ 154.36, 74.41, 67.04, 43.88 ppm.

4-phenyl-1,3-dioxolan-2-one
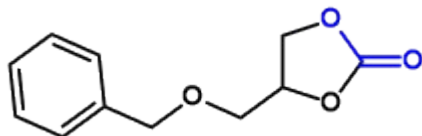**^{1}H NMR (300 MHz, CDCl₃)**: δ 7.48-7.34 (m, 5H), 5.71-5.66 (t, 1H), 4.84-4.78 (t, 1H), 4.38-4.32 (t, 1H) ppm;
^{13}C NMR (75 MHz, CDCl₃): δ 154.20, 135.37, 129.35, 128.86, 125.52, 78.09, 71.33 ppm.

4-(phenoxymethyl)-1,3-dioxolan-2-one
^{1}H NMR (300 MHz, CDCl₃): δ 7.33-7.29 (t, 2H), 7.04-7.00 (t, 1H), 6.92-6.90 (d, 2H), 5.06-5.00 (m, 1H), 4.64-4.59 (t, 1H), 4.56-4.52 (t, 1H), 4.26-4.22 (dd, 1H), 4.16-4.13 (dd, 1H) ppm;
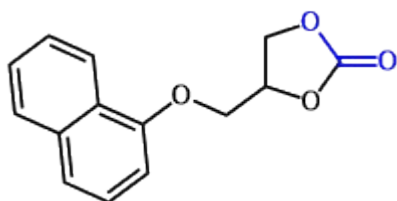**^{13}C NMR (75 MHz, CDCl₃)**: δ 157.85, 154.80, 129.82, 121.11, 114.71, 74.23, 66.96, 66.36 ppm.

4-((benzyloxy)methyl)-1,3-dioxolan-2-one
¹H NMR (300 MHz, CDCl₃): δ 7.39-7.29 (m, 5H), 4.84-4.78 (m, 1H), 4.63-4.55 (m, 2H), 4.49-4.45 (t, 1H), 4.40-4.36 (m, 1H), 3.73-3.69 (dd, 1H), 3.63-3.59 (dd, 1H) ppm;
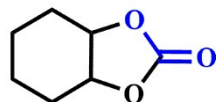**¹³C NMR (75 MHz, CDCl₃)**: δ 155.06, 137.16, 128.67, 128.17, 127.84, 75.11, 73.77, 68.91, 66.38 ppm.

4-((naphthalen-1-yloxy)methyl)-1,3-dioxolan-2-one
¹H NMR (400 MHz, CDCl₃): δ 8.17-8.15 (t, 1H), 7.82-7.80 (t, 1H), 7.52-7.49 (m, 3H), 7.38-7.35 (t, 1H) 6.79-6.77 (d, 1H), 5.14 (s, 1H), 4.68-4.66 (m, 2H), 4.44-4.41 (dd, 1H), 4.29-4.26 (dd, 1H) ppm;
¹³C NMR (101 MHz, CDCl₃): δ 154.88, 153.53, 134.64, 127.68, 126.02, 126.02, 125.60, 125.37, 121.82, 121.66, 104.98, 74.30, 67.38, 66.45 ppm.
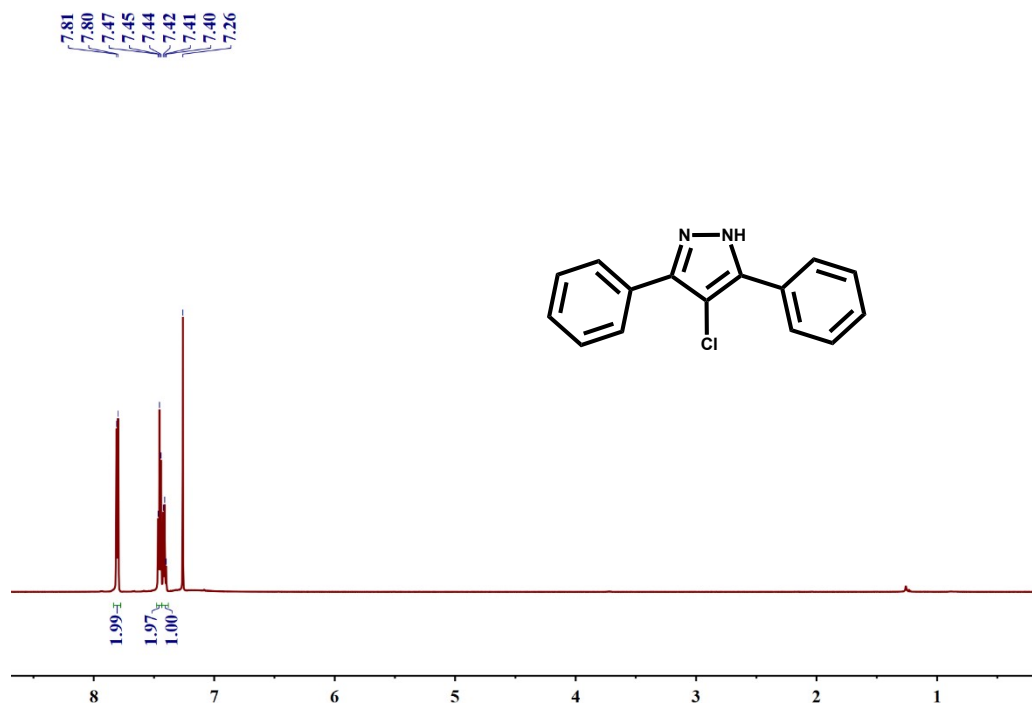

Hexahydrobenzo[*d*][1,3]dioxol-2-one
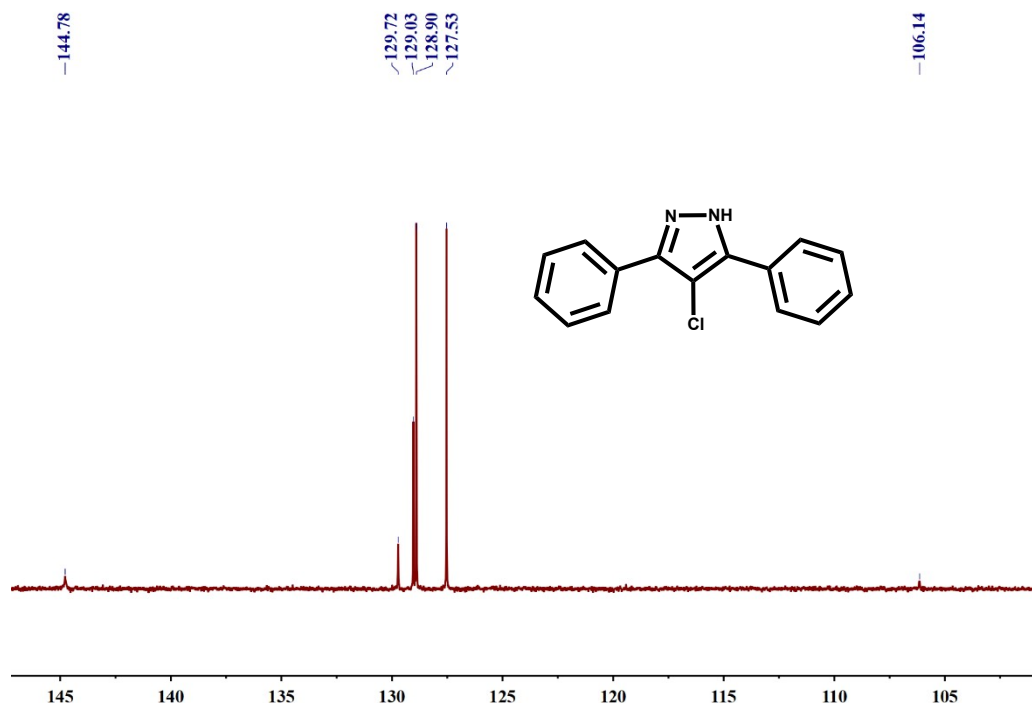**¹H NMR (400 MHz, CDCl₃)**: δ 4.66 (s, 2H), 1.86 (s, 4H), 1.59-1.54(m, 2H), 1.43-1.38 (m, 2H);
¹³C NMR (101 MHz, CDCl₃): δ 155.45, 75.82, 26.76, 19.16 ppm.

¹H NMR and ¹³C NMR Spectra of 4-Chloro-3,5-Diphenylpyrazole
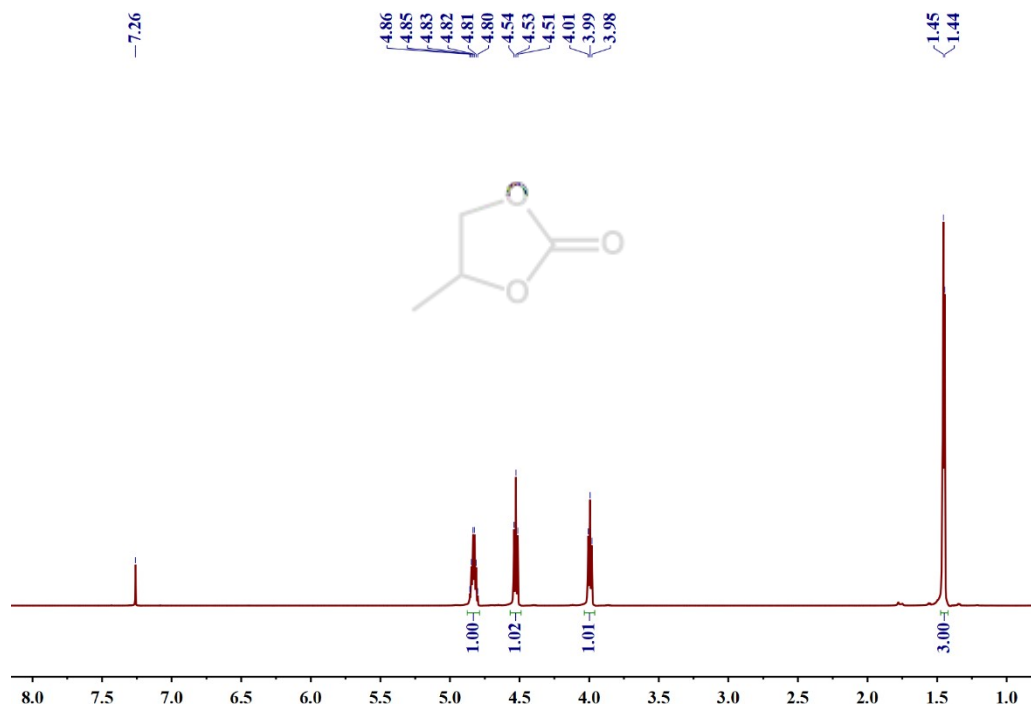
¹H NMR (CDCl₃, 400 MHz)

7.81
7.80
7.47
7.45
7.44
7.42
7.41
7.40
7.26

1.99
1.97
1.00

8 7 6 5 4 3 2 1

¹³C NMR (CDCl₃, 101 MHz)

144.78
129.72
129.03
128.90
127.53
106.14

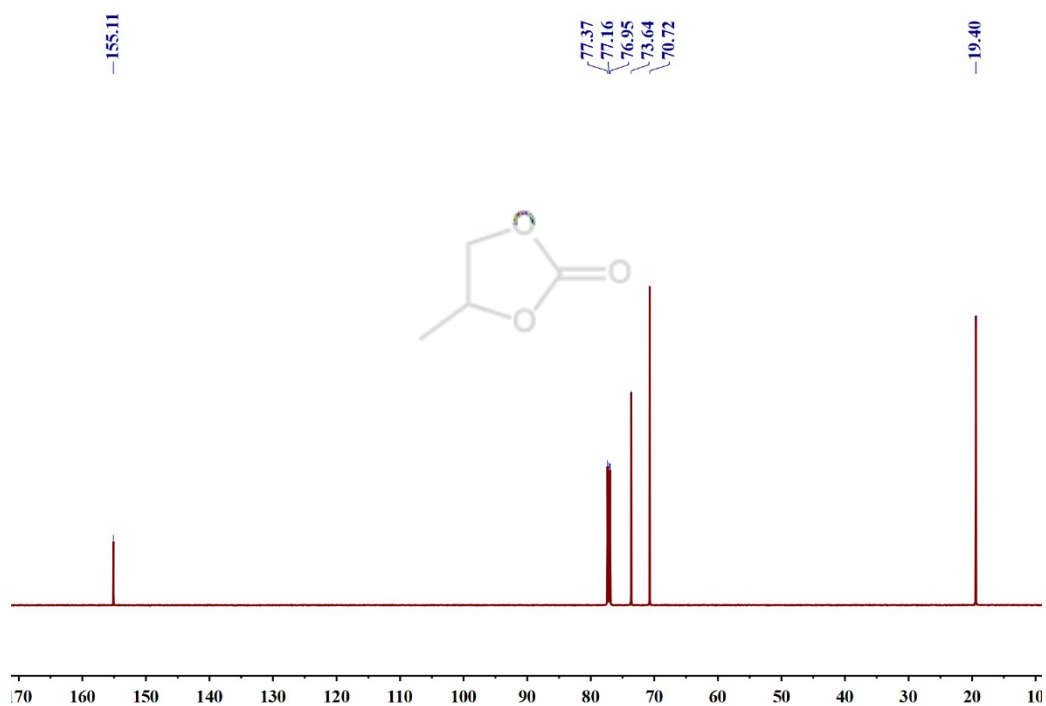145 140 135 130 125 120 115 110 105

¹H NMR and ¹³C NMR Spectra of Products

4-methyl-1,3-dioxolan-2-one
¹H NMR (CDCl₃, 400 MHz)

¹³C NMR (CDCl₃, 101 MHz)

4-(chloromethyl)-1,3-dioxolan-2-one
^{1}H NMR (CDCl$_3$, 300 MHz)
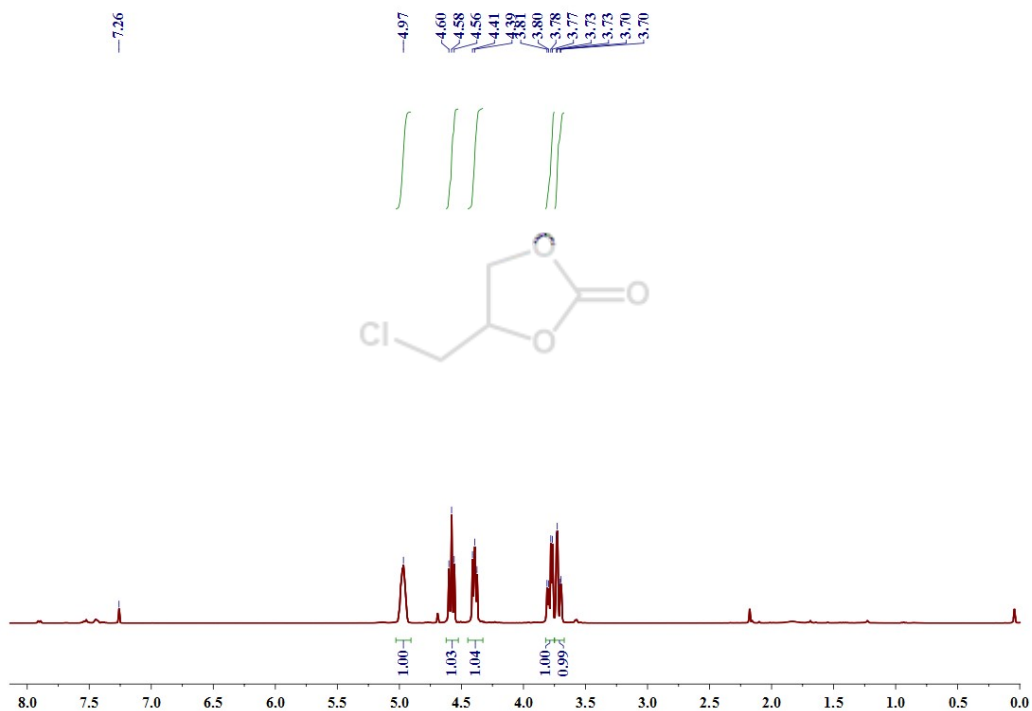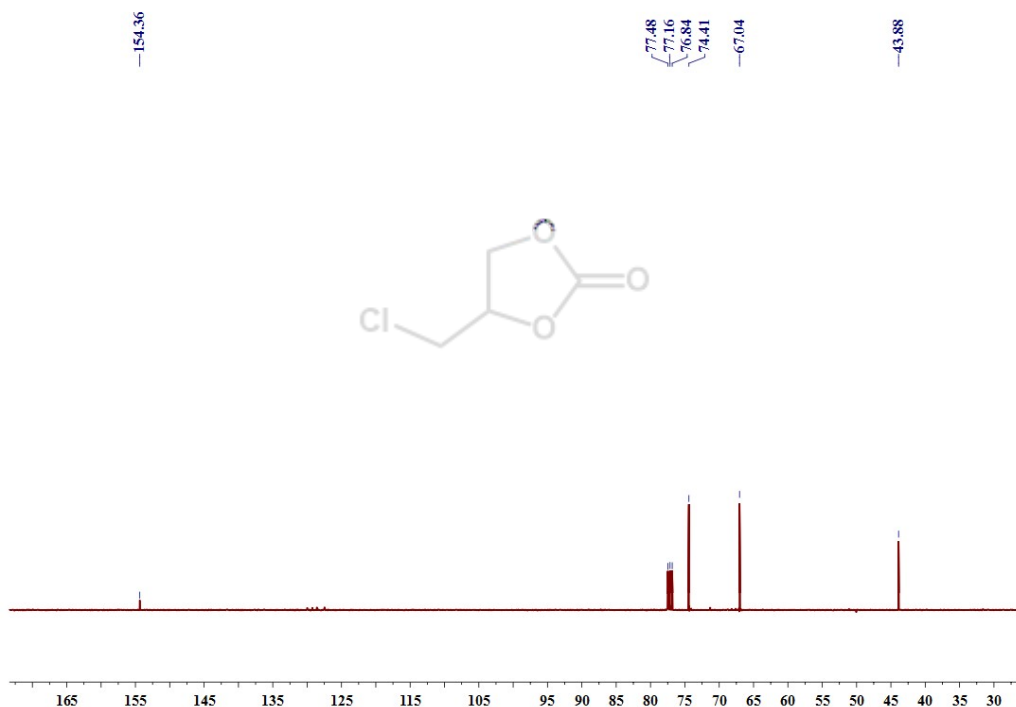
^{13}C NMR (CDCl$_3$, 75 MHz)

4-phenyl-1,3-dioxolan-2-one
^{1}H NMR (CDCl$_3$, 300 MHz)
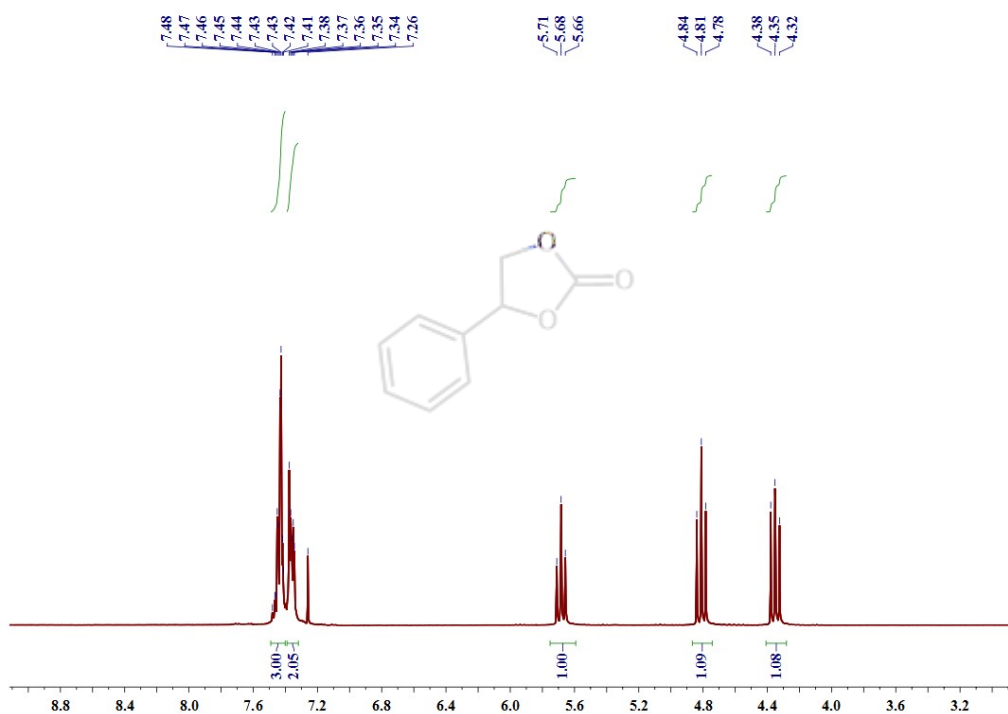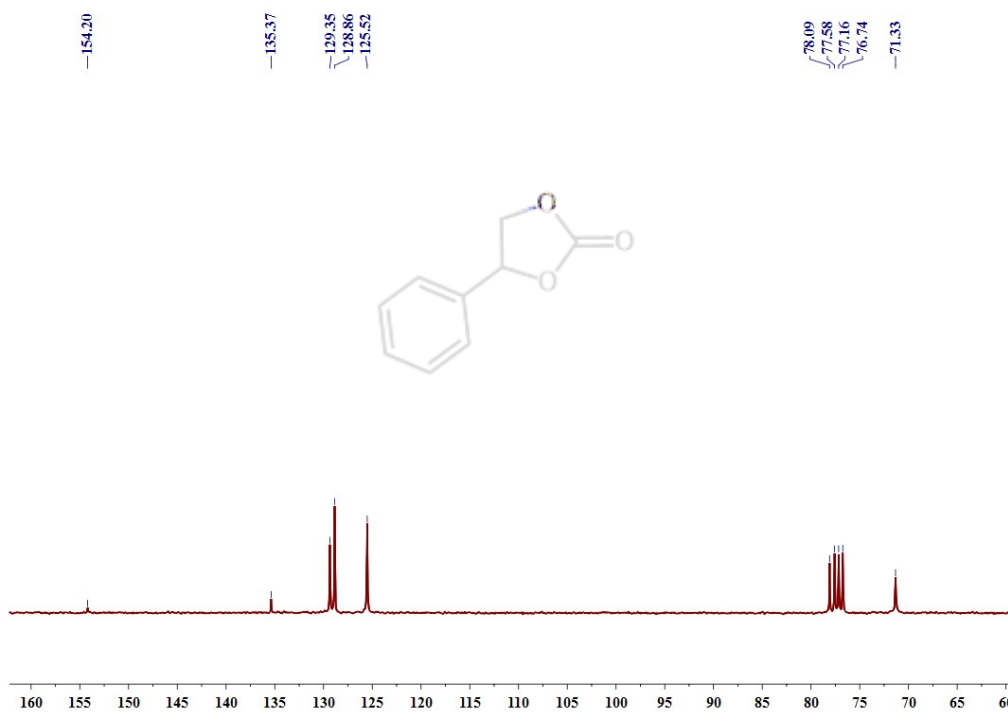
^{13}C NMR (CDCl$_3$, 75 MHz)

4-(phenoxymethyl)-1,3-dioxolan-2-one
^{1}H NMR (CDCl$_3$, 300 MHz)

7.33, 7.31, 7.29, 7.26, 7.04, 7.02, 7.00, 6.92, 6.90
5.06, 5.05, 5.04, 5.03, 5.01, 5.00
4.62, 4.56, 4.54, 4.26, 4.25, 4.23, 4.22, 4.16, 4.15, 4.13, 4.13

2.11 0.95 1.94 1.00 1.06 1.02 0.99 0.99

9.0 8.6 8.2 7.8 7.4 7.0 6.6 6.2 5.8 5.4 5.0 4.6 4.2 3.8 3.4 3.0

^{13}C NMR (CDCl$_3$, 75 MHz)

157.85, 154.80, 129.82, 122.11, 114.71, 77.48, 77.16, 76.84, 74.23, 66.96, 66.36

170 165 160 155 150 145 140 135 130 125 120 115 110 105 100 95 90 85 80 75 70 65 60 55
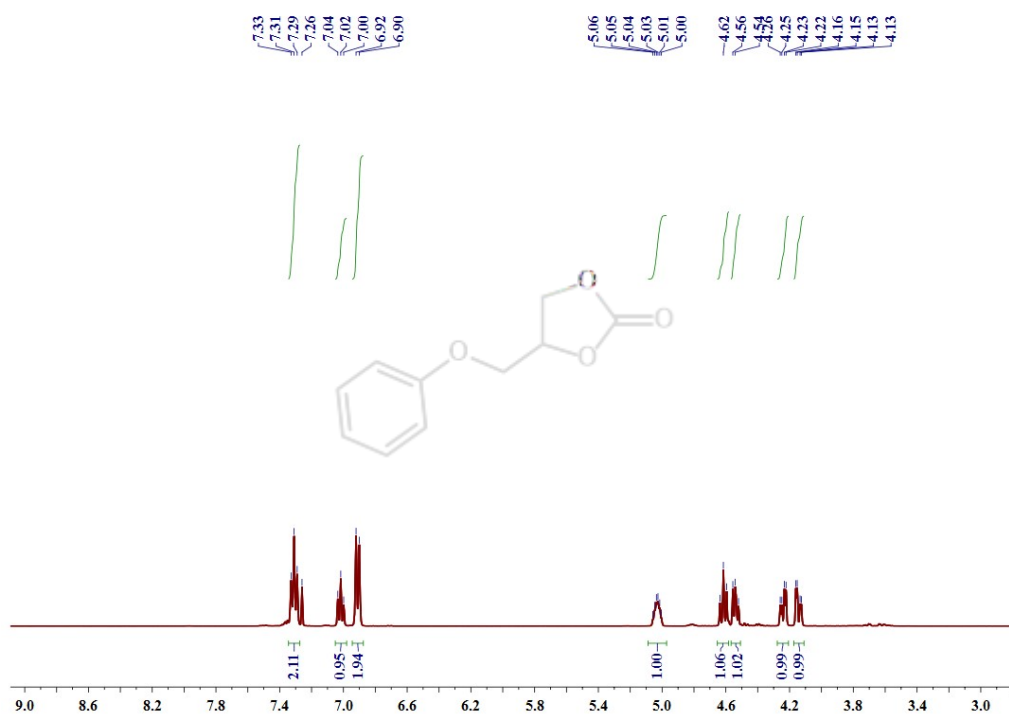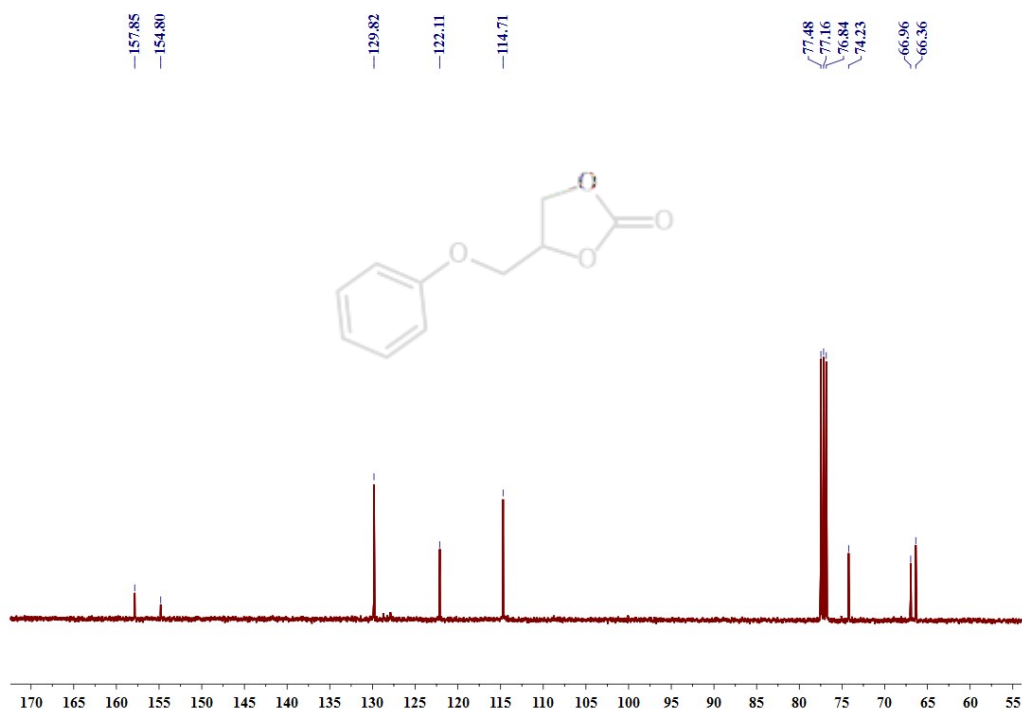
4-((benzyloxy)methyl)-1,3-dioxolan-2-one
^{1}H NMR (300 MHz, CDCl$_3$)
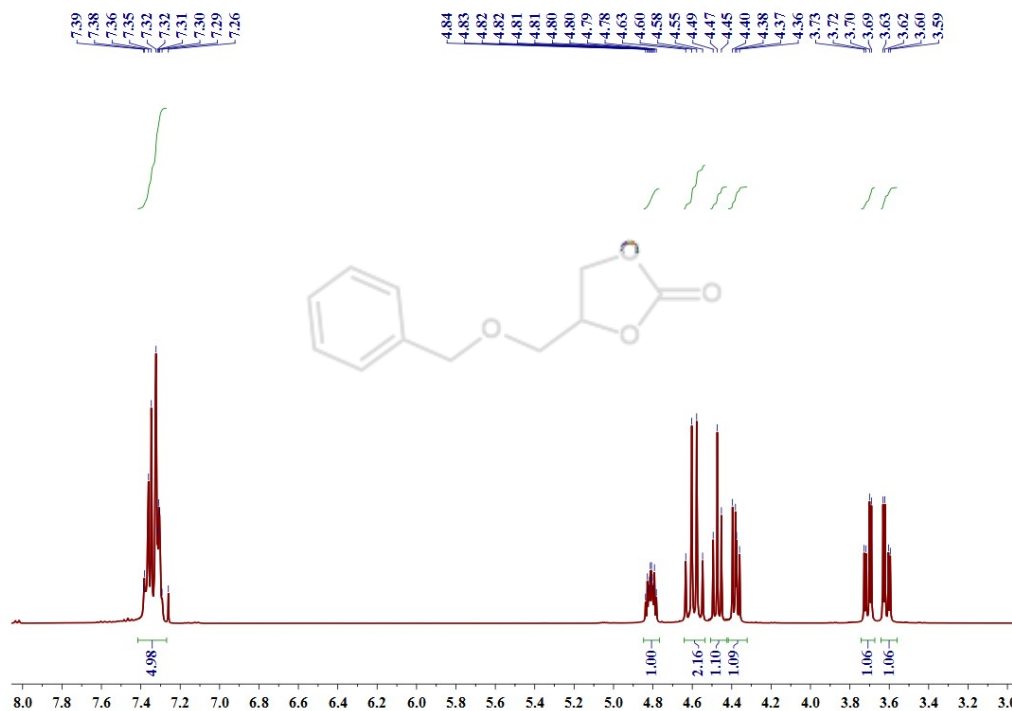
^{13}C NMR (75 MHz, CDCl$_3$)

4-((naphthalen-1-yloxy)methyl)-1,3-dioxolan-2-one
^{1}H NMR (CDCl$_3$, 400 MHz)

8.17 8.16 8.15 7.82 7.81 7.80 7.52 7.51 7.49 7.38 7.37 7.35 7.26 6.79 6.77
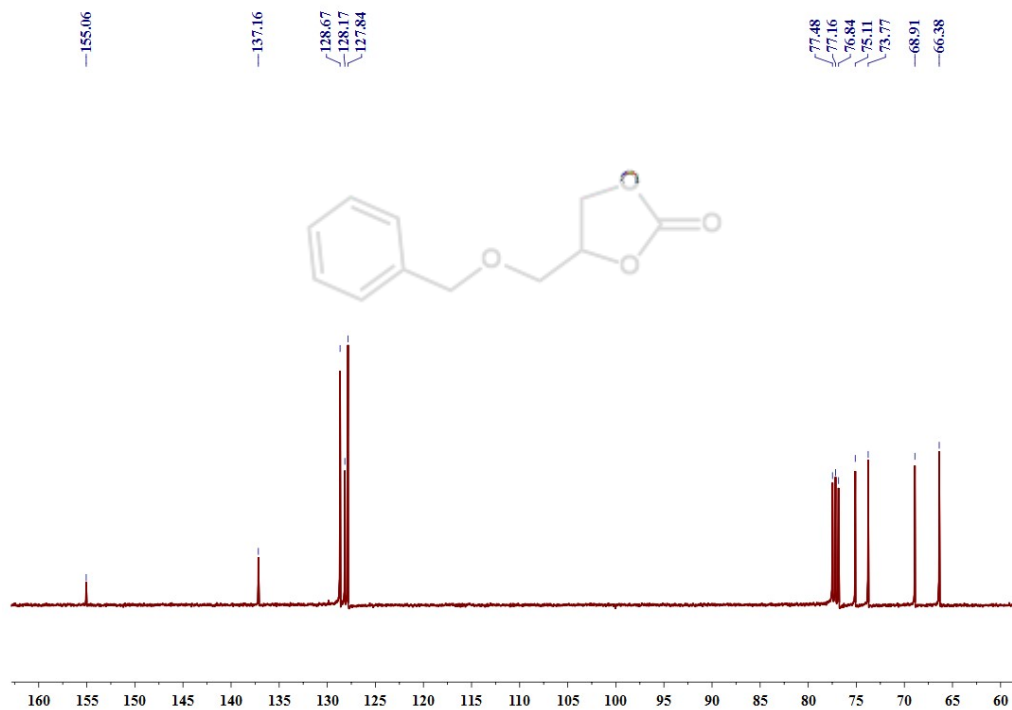5.14
4.68 4.66 4.44 4.44 4.42 4.41 4.29 4.26

1.00 1.01 3.05 1.02 1.00 1.05 2.09 1.05 1.03

9.0 8.5 8.0 7.5 7.0 6.5 6.0 5.5 5.0 4.5 4.0 3.5 3.0 2.5 2.0

^{13}C NMR (CDCl$_3$, 101 MHz)

154.88 153.53
134.64 127.68 126.94 126.02 125.60 125.37 121.82 121.66
104.98
77.48 77.16 76.84 74.30 67.38 66.45

170 160 150 140 130 120 110 100 90 80 70 60 50
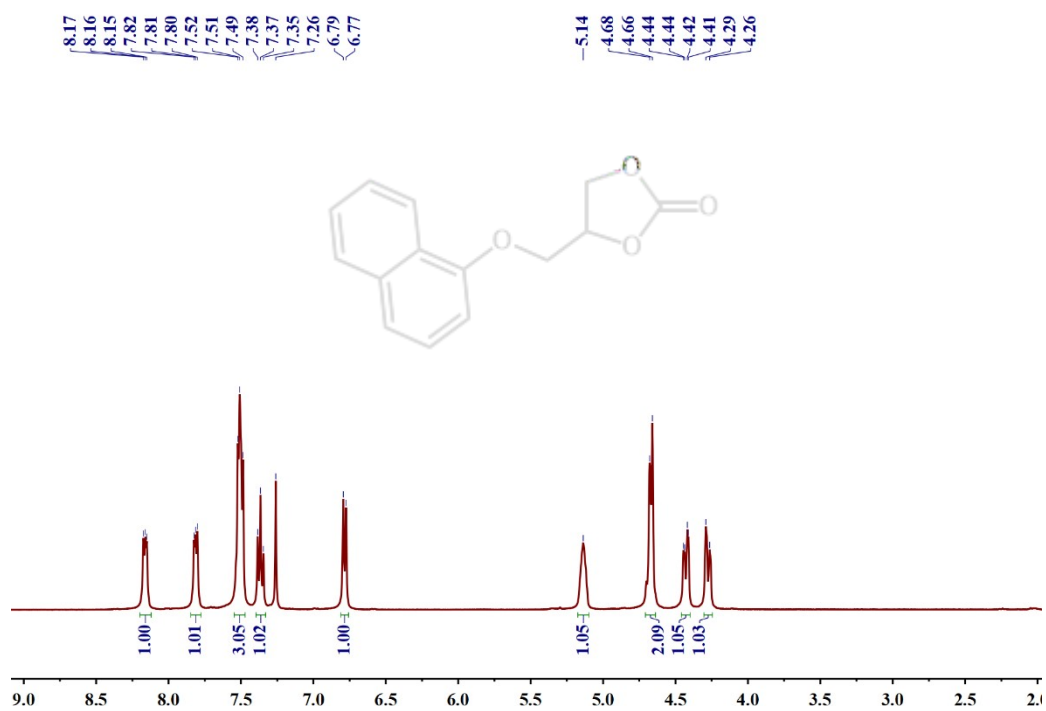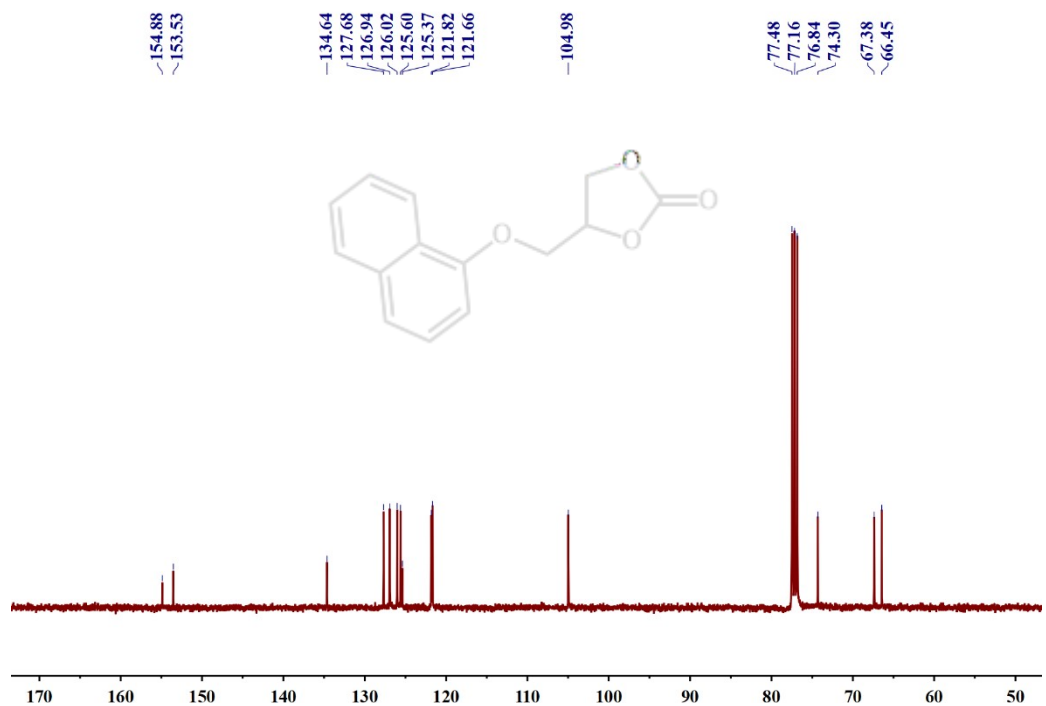
Hexahydrobenzo[*d*][1,3]dioxol-2-one
^{1}H NMR (CDCl$_3$, 400 MHz)
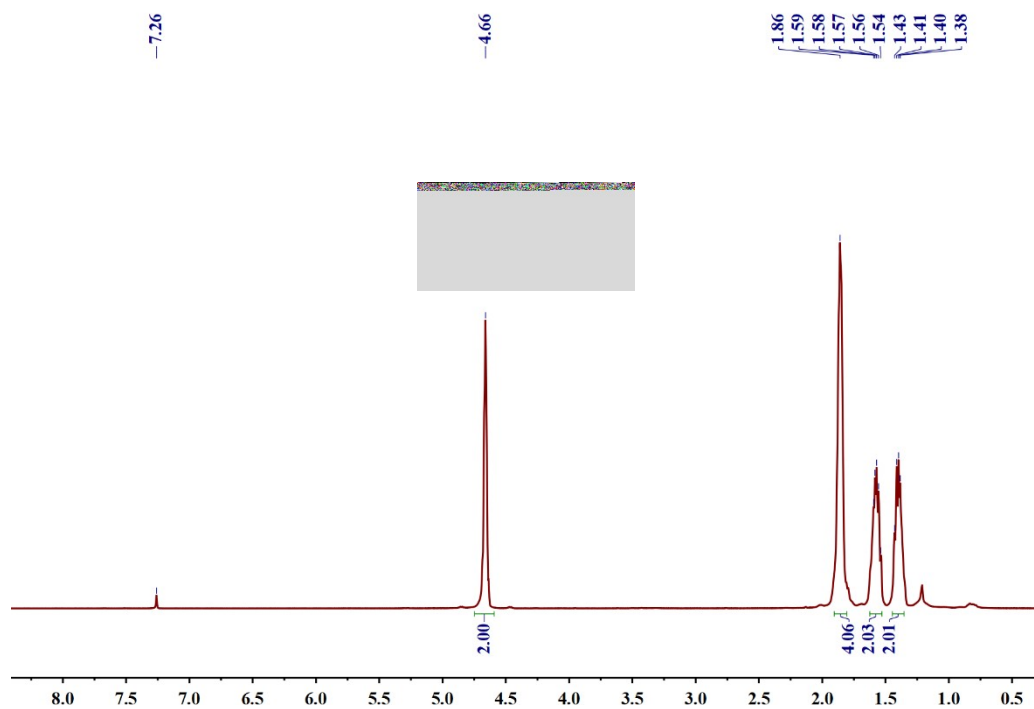
^{13}C NMR (CDCl$_3$, 101 MHz)
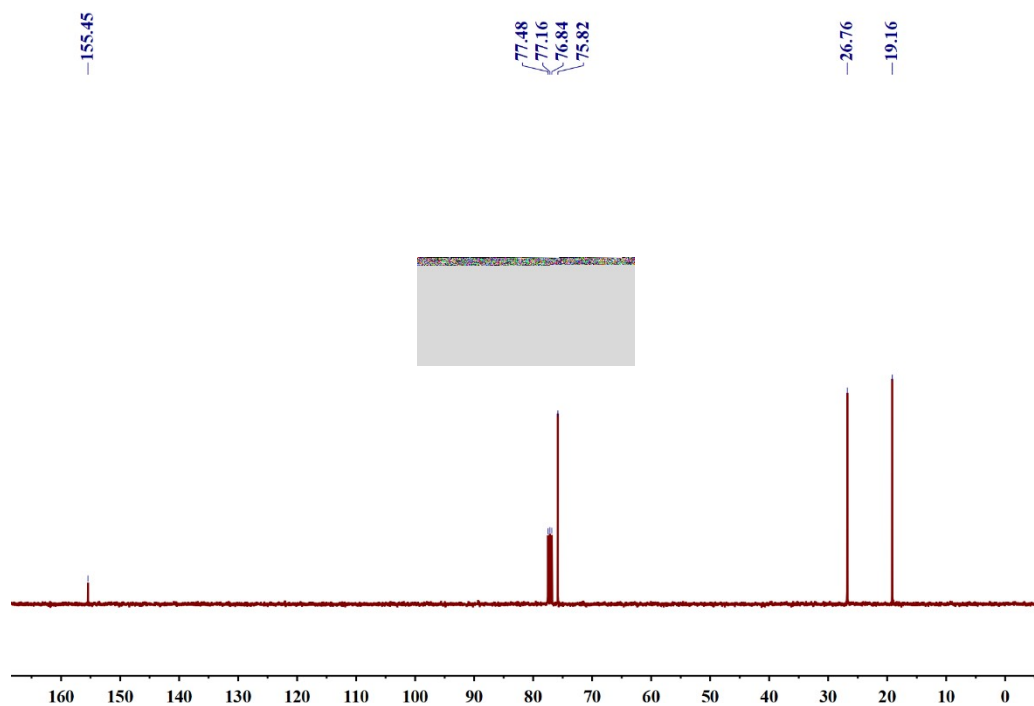
Reference

1   J. Ackermann, F. Meyer, E. Kaifer and H. Pritzkow, *Chem. Eur. J.*, 2002, **8**, 247–258.

2   W. A. A. Isawi, M. Zeller and G. Mezei, *Cryst. Growth Des.*, 2022, **22**, 1398–1411.

3   S. K. Dey, T. S. M. Abedin, L. N. Dawe, S. S. Tandon, J. L. Collins, L. K. Thompson, A. V. Postnikov, M. S. Alam and Paul Müller, *Inorg. Chem.*, 2007, **46**, 7767–7781.

4   C. R. Murdock and D. M. Jenkins, *J. Am. Chem. Soc.*, 2014, **136**, 10983–10988.

5   J. Ying, C. Sun, L. Jin, A. Tian and X. Wang, *CrystEngComm*, 2021, **23**, 5385–5396.

6   A. B. Lysenko, O. A. Bondar, G. A. Senchyk, E. B. Rusanov, M. Srebro-Hooper, J. Hooper, K. Prsa, K. W. Krämer, S. Decurtins, O. Waldmann and S.-X. Liu, *Inorg. Chem.*, 2018, **57**, 6076–6083

7   M. K. Melvin, B. W. Skelton, P. K. Eggers and C. L. Raston, *CrystEngComm*, 2022, **24**, 57–69.

8   E.-C. Yang, Z.-Y. Liu, S.-H. Chen, Y.-H. Su, Y.-Y. Zhang and X.-J. Zhao, *Dalton Trans.*, 2015, **44**, 3190–3199.

9   Y. Zhou, H. Chen, X. Gu and X. Bian, *J. Mol. Struct.*, 2022, **1254**, 132324.

10 J.-H. Chen, C.-H. Deng, S. Fang, J.-G. Ma and P. Cheng, *Green. Chem.*, 2018, **20**, 989–996.

11 S.-S. Yu, X.-H. Liu, J.-G. Ma, Z. Niu and P. Cheng, *J. CO_2 Util.*, 2016, **14**, 122–125.

12 F. Zhou, S.-L. Xie, X.-T. Gao, R. Zhang, C.-H. Wang, G.-Q. Yin and J. Zhou, *Green. Chem.*, 2017, **19**, 3908–3915.

13 M. Liu, X. Li, X. Lin, L. Liang, X. Gao and J. Sun, *J. Mol. Catal. A: Chem.*, 2016, **412**, 20–26.

14 F. Cruz-Martinez, J. Martinez, M. A. Gaona, J. Fernandez-Baeza, L. F. Sanchez-Barba, A. M. Rodriguez, J. A. Castro-Osma, A. Otero and A. Lara-Sanchez, *ACS Sustainable Chem. Eng.*, 2018, **6**, 5322–5332.

15 N. H. Kim, E. Y. Seong, J. H. Kim, S. H. Lee, K. H. Ahn and E. J. Kang, *J. CO_2 Util.*, 2019, **34**, 516–521.

16 Y.-L. Hu, M. Lu and X.-L. Yang, *RSC Adv.*, 2015, **5**, 67886–67891.

17 J. Martínez, J. Fernandez-Baeza, L. F. Sánchez-Barba, J.-A. Castro-Osma, A. Lar a-Sánchez and A. Otero, *ChemSusChem*, 2017, **10**, 2886–2890.

18 J. Sun, W..Cheng, Z. Yang, J. Wang, T. Xu, J. Xin and S. Zhang, *Green Chem*, 2014, **16**, 3071–3078.